Eccentric Phenomena at Liquid Mercury Electrode/Solution Interfaces: Upward, Downward, and Circular Motions

Md. Mominul Islam, Takeyoshi Okajima, and Takeo Ohsaka*

Department of Electronic Chemistry, Interdisciplinary Graduate School of Science and Engineering, Tokyo Institute of Technology, Mail Box G1-5, 4259 Nagatsuta, Midori-ku, Yokohama 226-8502, Japan

Received: January 26, 2006

The present paper describes a visualization of unidirectional and circular motions triggered by an electrochemical redox reaction at a charged, bent, and streamed liquid electrode/liquid solution interface. The novel circular motion that induces a conversion of electrochemical energy into mechanical energy could be visualized for the first time at a hanging mercury drop electrode (HMDE)/dimethyl sulfoxide (DMSO) solution interface via the electrochromic reaction of 2,1,3-benzothiadiazole (BTD) by using a CCD−color video camera. The observed motions are self-insisting in nature and are tunable into upward, downward, clockwise, and anticlockwise ones by an appropriate choice of the experimental conditions. This circular motion is visualized for the first time as the cause of the well-known cyclic voltammetric anodic current oscillation at the HMDE. Several small perturbations, for example, surface tension, surface motion, bulk motion, diffusional mass transport, and surface electrochemical potential are considered to be endlessly amplified by their coupling in a cyclic chain, resulting in such macroscopic motions at the electrode/solution interface. All of the phenomena can be explained on the basis of the modern theory proposed by Aogaki et al. (*Electrochim. Acta* **1978**, *23*, 867) for the polarographic streaming maxima of the first kind.

Introduction

Instabilities that happen without any apparent cause (but actually result from the gravitational force) are often observed in many natural systems, for example, the spiral motion in the smock formed during the burning of cellulosic materials (or boiling of water), swirling of water in the outlet of a sink (or bathtub), vortex in the fluid flow, and circular motion of hurricanes and tornadoes.[1−4] On the other hand, the electrochemical instabilities (e.g., current and potential oscillations) are known to be originated generally from the combined microscopic physicochemical perturbations at the electrode/solution interface due to the different interfacial changes, for example, electrocrystallization, chemical reaction at the electrode vicinity, adsorption, passivation−activation and dissolution (i.e., corrosion) of the electrode surface, and so on.[5−13] Another familiar electrochemical instability is the polarographic streaming phenomena of a hanging mercury drop electrode (HMDE) that results from the dissimilar surface tension of the liquid mercury drop and that has been hitherto presumed to induce a cyclic voltammetric anodic current oscillation (CVACO),[13−28] but the mechanisms of the CVACO presented on the basis of the classical theories of the polarographic streaming phenomena are still ambiguous.[13,15,20,21,26,27]

In the present study, we have visualized for the first time that a circular motion at the HMDE/solution interface causes CVACO that was first reported in 1964.[14] The observed circular motion seems to induce a conversion of electrochemical energy into mechanical energy and should be explored as a novel concept in the field of electrochemical instability at a charged liquid surface (mercury)/liquid electrolyte interface. We anticipate that this circular motion could advance the visual knowledge of the self-insisting instability in the other systems involving the charged interface (e.g., the vortices in electroosmotic flow,[2] instabilities in the fluid flow of biochannel or biochips[2,3]) and that a suitable fabrication of this novel circular motion may tender its application, for example, as a microtransducer for a mechanical amplification system triggered by an electrochemical redox reaction.

The upward and downward streaming phenomena at the HMDE/solution interface that are well-known conceptually[15,26−29] but not observed directly except for a few cases[27−35] and a novel circular motion were typically visualized via the electrochromism of 2,1,3-benzothiadiazole (BTD) in dimethyl sulfoxide (DMSO) solution[28] by using a CCD−color video camera involving a home-assembled optoelectrochemical system. Furthermore, the CCD−video measurements were extensively carried out with a hemispherical mercury pool electrode (HSMPE) to confirm the direction of the observed circular motion. The mechanism of the CVACO was also discussed.

Experimental Section

Reagents. Dimethyl sulfoxide (DMSO) and *N*,*N*-dimethylformamide (DMF) as solvents, and tetraethylammonium perchlorate (TEAP) as electrolyte, were purchased from Kanto Chemical Co., Inc. Prior to use, the solvents were dried by an activated molecular sieve (4A 1/16, Wako Pure Chemicals Industries). Azobenzene and tris(2,2′-bipyridine)ruthenium(II) dichloride hexahydrate were purchased from Kanto Chemical Co., Inc. and Aldrich, respectively. All of the chemicals were of reagent grade and used without further purifications.

Apparatus and Procedures. The optoelectrochemical system consisted of two parts: electrochemical and optical.[28] The electrochemical part was a two-compartment, three-electrode system in which a spherical HMDE (model CGME 900,

* To whom correspondence should be addressed. E-mail address: ohsaka@echem.titech.ac.jp.

10.1021/jp060558e CCC: $33.50
Published on Web 04/11/2006

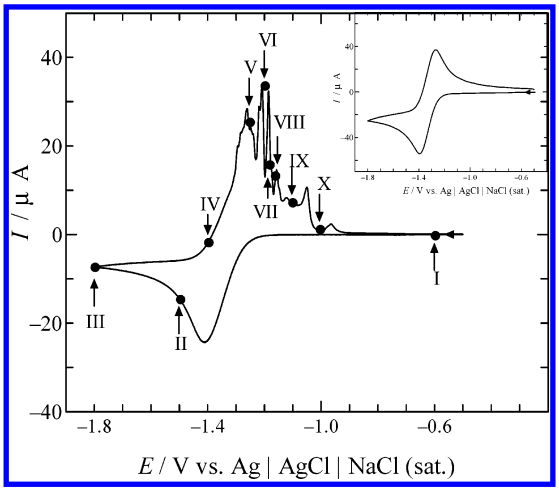

Figure 1. CVs obtained for the redox reaction of BTD/BTD$^{\bullet-}$ couple at HMDE and Pt electrode (inset) in DMSO solution containing 0.1 M TEAP and 5 mM BTD. Potential scan rate: 0.1 V s^{-1}. The filled circles and arrows indicate the potentials where the images shown in Figure 2 were captured and the Roman numbers represent their captured order.

Bioanalytical Systems, Inc. (BAS), diameter (ϕ) = 0.76 mm) or a homemade hemispherical mercury pool electrode (HSMPE, ϕ = 2 mm) or a spherical platinum (Pt, ϕ = ca. 1.4 mm) working electrode, a silver (Ag)/silver chloride (AgCl)/saturated sodium chloride (NaCl (saturated)) reference electrode or an Ag wire quasi-reference electrode and a spiral Pt wire counter electrode were used. HSMPE is a mercury pool placed into a cylindrical cavity (ϕ = 2 mm) on a Teflon support for which the electrical contact was made with a Teflon-seated Pt wire. The working electrode compartment, which is a rectangular quartz vessel containing working and counter electrodes, and the reference electrode compartment were connected by a salt bridge filled with the solution of interest. The voltammetric measurements were performed by using a computer-controlled electrochemical analyzer (Model 50W, BAS). The optical part was comprised of a CCD−color video camera with a camera probe (Model VC-HRM50Z, OMRON Co., Japan) and a controller (Model VC-1000 3D digital fine scope, OMRON Co., Japan) with which a timer (Model VTG-33, FOR-A Co. Ltd., Japan) was connected. Further, the timer was interfaced to a personal computer via a modem. In cases of the HMDE and Pt electrode, the videos were measured from the side-view arrangement (the detail in our previous paper[28]), while the video at HSMPE was captured from its upper position. The videos of the HMDE, HSMPE, and Pt electrode were captured on the best of focus at 250-, 50-, and 125-times magnification, respectively. All the measurements were carried out at room temperature (25 ± 2 °C) under N_2 atmosphere.

Results and Discussion

Figure 1 shows the cyclic voltammograms (CVs) obtained for the redox reaction of BTD at HMDE and spherical Pt electrode (inset) in DMSO solution containing 0.1 M tetraethylammonium perchlorate (TEAP). The CV obtained at the Pt electrode shows a couple of well-defined cathodic and anodic peaks at potentials of −1.39 and −1.27 V, respectively. These peaks correspond to the one-electron reduction of colorless BTD to pink BTD anion radical (BTD$^{\bullet-}$) and the oxidation of BTD$^{\bullet-}$ to BTD.[26,28] The cathodic peaks obtained at the HMDE and Pt electrode were similar in their shapes and potentials, while current-oscillating and smooth anodic waves were observed at HMDE and Pt electrode, respectively. Similarly to the other reported redox reactions at the HMDE,[13−27] the characteristic CVACO was observed in the present case as well. Our group has studied CVACO at the HMDE in recent years,[13,22−27] and the characteristics of CVACO are as follows: it does not occur (i) at conventional solid electrodes (e.g., Pt, gold, and glassy carbon electrodes), (ii) at potentials more positive than the potential of zero charge (PZC), (iii) at faster potential scan rates, and (iv) in the solution containing lower and higher concentrations of redox species and electrolyte, respectively. In the present study, during the measurement of the CVs shown in Figure 1, CCD−color videos of the Pt electrode and the HMDE were simultaneously captured to follow the streaming phenomena at the electrode/solution interfaces via the electrochromism of the BTD/BTD$^{\bullet-}$ redox couple.

In the video of the HMDE captured during the reduction process, the electrogenerated pink BTD$^{\bullet-}$ was observed to inhomogeneously diffuse in the vicinity of the neck of the HMDE (see Figure 4b). On the other hand, a circular motion of the pink BTD$^{\bullet-}$ was found to take place accompanying the current oscillation during the reoxidation process of BTD$^{\bullet-}$ to BTD (video A). The viewing of such inhomogeneous diffusion and the circular motion of the pink BTD$^{\bullet-}$ seems to be interesting. Figure 2 represents the typical CCD−color video images of the HMDE captured during the CV measurement. The digits on each frame signify the time required to scan up to the potential marked by each arrow on the CV shown in Figure 1. Strictly speaking, each image visualizes the extent of physical and electrochemical changes of the HMDE and its vicinity at the respective potentials. The image I captured at −0.6 V, where no electrochemical reaction takes place, was taken as the reference image to all the others (i.e., images II−X). As can be seen from the images II and III, the density of the pink BTD$^{\bullet-}$ gradually increases as the electrode potential is scanned to the negative direction of potential, and the formation of the pink BTD$^{\bullet-}$ more predominantly proceeds in the vicinity of the neck than that of the bottom of the HMDE. This inhomogeneous distribution of the pink BTD$^{\bullet-}$ obviously resulted from the upward streaming phenomena.[15,26−29] On the other hand, the images V−IX, which were captured during the reoxidation process of BTD$^{\bullet-}$, show that the density of the pink BTD$^{\bullet-}$ in the vicinity of the neck gradually and inhomogeneously decreases. This can be clearly observed in images V and VI, where the pink color around the base of the capillary of the HMDE pales quickly and the color density surrounding the HMDE sphere remains almost constant. This change of the colored BTD$^{\bullet-}$ distribution indicates the existence of the downward streaming of the HMDE surface and its adjoining solution.[15,26−29]

The creation of the so-called circular motion can be clearly traced by reviewing successively the typical images VI−X (or in video A).[36] In image VI, the pink BTD$^{\bullet-}$ species are distributed almost homogeneously around the HMDE sphere. In image VII, the color of the solution at the right-hand side of the HMDE sphere is slightly deeper than that of its left-hand side, and in image VIII, most of the pink BTD$^{\bullet-}$ species are moved to the right-hand side of the HMDE sphere, while the reverse situation can be seen in image IX. Such a movement of the pink BTD$^{\bullet-}$ from the right-hand side to the left-hand side was observed to be repeated many times (ca. 5 times). Here, it should be noted that a "threshold" potential at which such a circular motion begins to take place during the anodic potential scan was found to be ca. −1.2 V. The analysis of the original video data and its consecutive separated images (the CCD−camera captured 30 frames/s) obtained during the occurrence

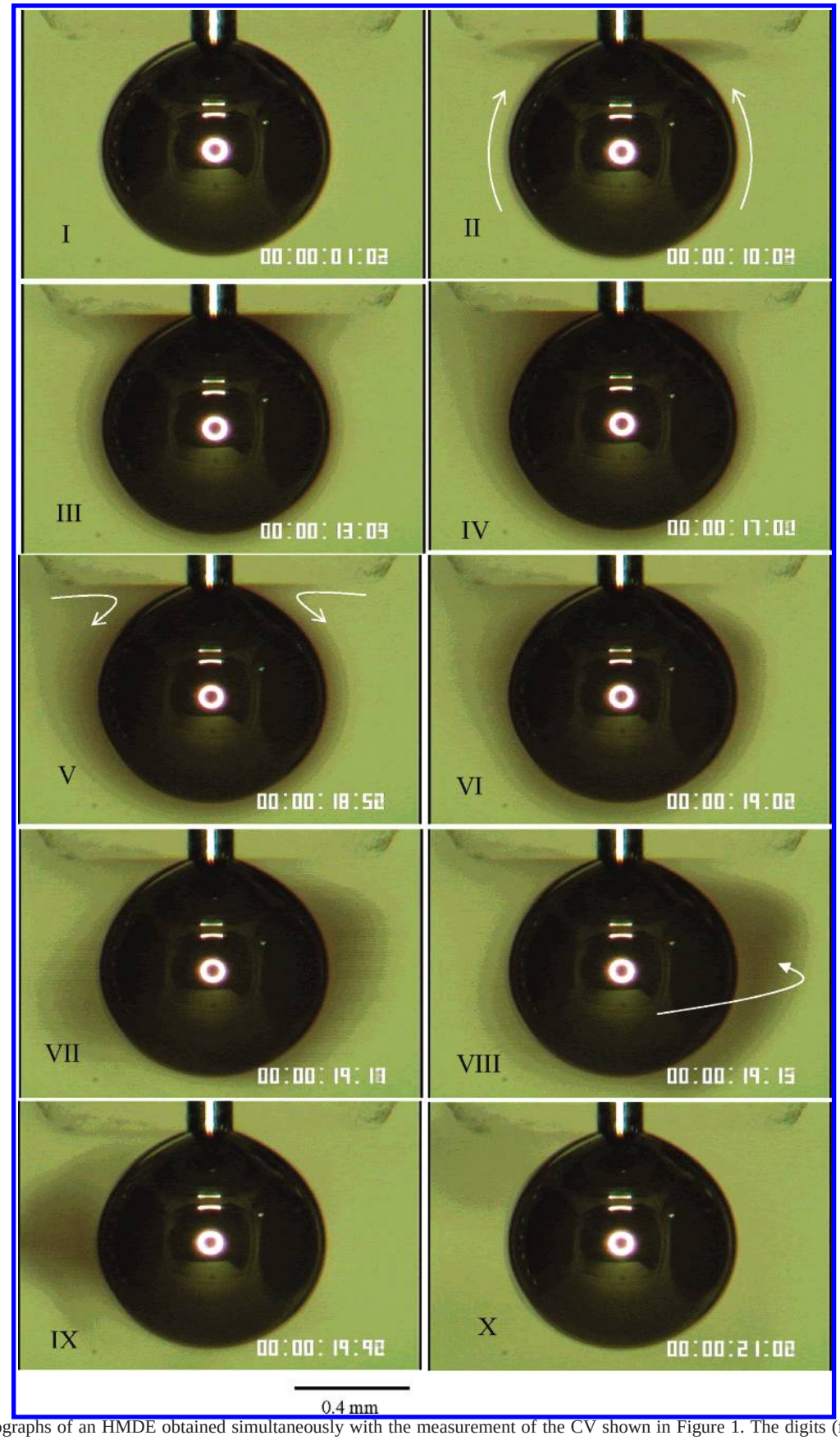

Figure 2. Photographs of an HMDE obtained simultaneously with the measurement of the CV shown in Figure 1. The digits (from the left-hand side; hour: minute: second: fraction of second) on each frame represents the time required to scan the potential up to each potential marked by arrow, as shown in Figure 1. The white spots on the each image are due to the flash from the light source arranged around the camera probe. The horizontal edge located above the mercury drop represents the base of the glass capillary dipped into the solution, and the vertical cylindrical column corresponds to the mercury column that is connected to the reservoir of mercury through the glass capillary. The arrows indicate the directions of movement of pink $BTD^{\bullet-}$. In the text, the neck and the bottom of the HMDE define the mercury surface attached to and far away from the glass capillary, respectively, shown in Figure 4.

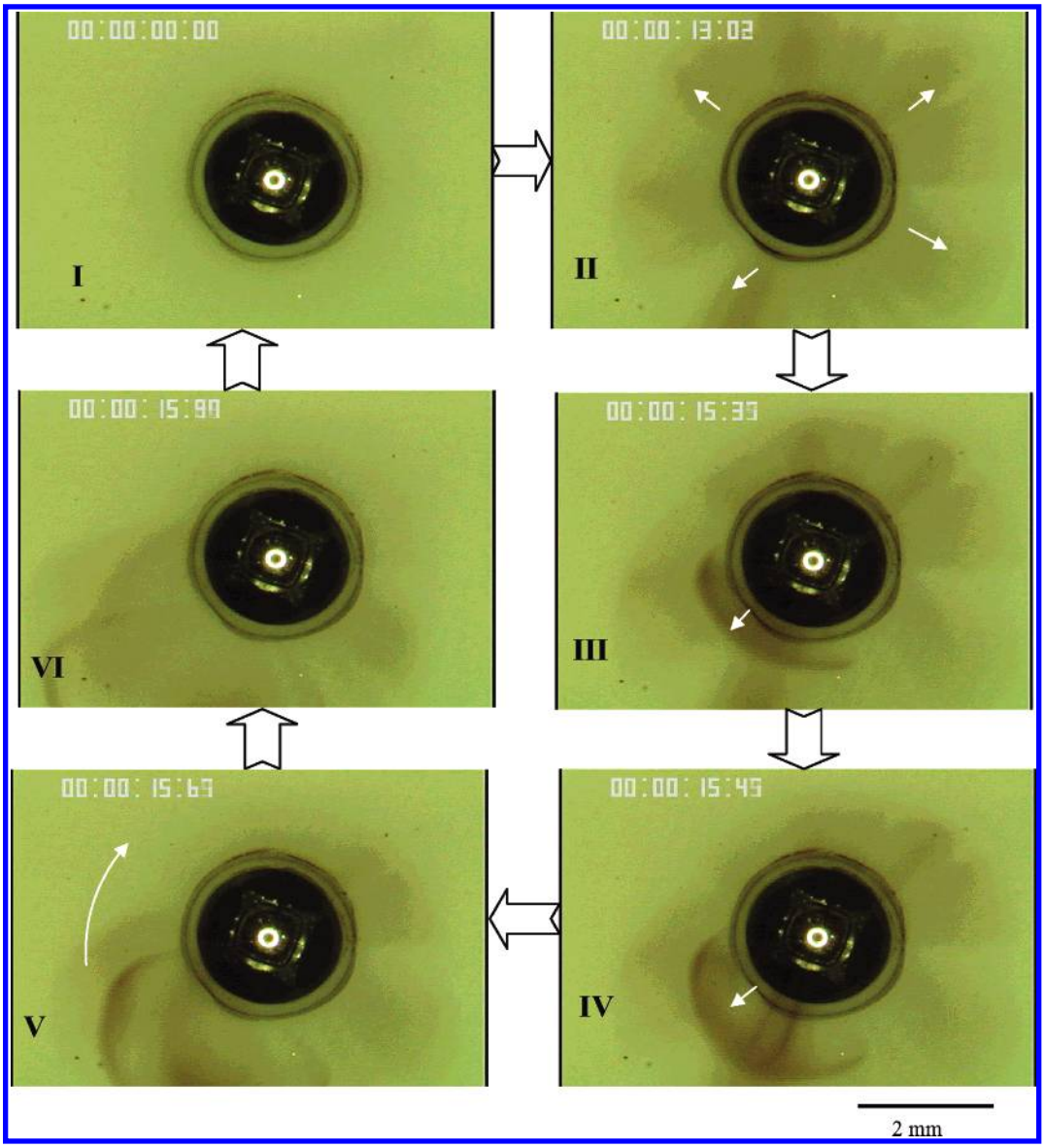

Figure 3. Photographs of the top view of an HSMPE captured during the measurement of a CV (in potential range of −0.5 → −1.6 → −0.5 V at potential scan rate: 0.1 V s^{-1}) in the same solution used for the measurement of the CV and the photographs shown in Figures 1 and 2, respectively. In the image I and other images, the observed black ring centering the mercury drop is due to the light reflection from the hemispherical mercury surface exposed vertically from the video camera. The arrows shown in images II, III (and IV), and V indicate the sunflowerlike symmetrical distribution, the jumping of the pink $BTD^{\bullet-}$ from the vicinity of the HSMPE to the bulk solution and a circular motion of the pink $BTD^{\bullet-}$ in solution, respectively. The outside arrows of each frame indicate the sequence of the images with their capturing time and situations of the pink $BTD^{\bullet-}$ in solution. The others features are similar to those explained in the caption of Figure 2.

of the circular motion revealed that the motion of the pink $BTD^{\bullet-}$ is a clockwise motion revolving around the HMDE sphere when we front on its bottom (discussed later), and the speed of rotation was estimated to be ca. 85 rpm. Finally, the pink $BTD^{\bullet-}$ species completely disappeared when the potential scan was completed, and the obtained image for this case was entirely identical to image I. Some additional features that can be viewed in the video and not clearly presented in the images are as follows: (i) the gradual shrinking and expansion of the HMDE sphere in the horizontal and vertical directions of the glass capillary axis, respectively, were observed during the reduction process of BTD to pink $BTD^{\bullet-}$, and interestingly, these were in the opposite during the oxidation process, and (ii) similarly to the previous interferometric observation,[27] a vigorous shaking of the HMDE sphere itself was also found during the reoxidation of $BTD^{\bullet-}$ to BTD.

The above-mentioned eccentric observation at the HMDE was made in a side-view mode.[28] By this observation, we can hardly tell about the direction of the circular motion, though the upward and downward streaming phenomena could be efficiently pictured by this mode. Instead, in a top-view mode of the HSMPE/DMSO solution interface during the redox reaction of the BTD/$BTD^{\bullet-}$ couple, we could clearly find the mentioned eccentric phenomena, especially the circular motion, even by eyes. Such observation at the HSMPE/DMSO solution interface was captured by using a CCD−video camera arranged at the top of the HSMPE. The obtained video clearly verifies the so-called clockwise circular motion of the pink $BTD^{\bullet-}$ around the mercury sphere (Figure 3). Figure 3 shows the typical top-view images of the HSMPE captured during the redox reaction of the BTD/$BTD^{\bullet-}$ couple in DMSO solution. In image I captured at −0.6 V, no color formation of the $BTD^{\bullet-}$ species should be expected because the electrode potential is much more positive than the reduction potential of BTD, and the observed situation in the vicinity electrode of the HSMPE is necessarily similar to that observed at the HMDE shown in image I of Figure 2. In

image II shown in Figure 3, which was captured after the completion of the reduction of BTD (the image I was captured at −1.4 V in the anodic cycle), a sunflower-like symmetrical distribution of the pink $BTD^{\bullet-}$ can be seen, indicating that the mercury surface and its adjoining solution moved from the center of the HSMPE toward the Teflon boundary of the hemispherical mercury drop. These observations reflect the upward streaming phenomenon of the HMDE (see images II and III in Figure 2) because the bottom of the HMDE corresponds to the center of the pool hemisphere. On the other hand, the pink $BTD^{\bullet-}$ distributed in the so-called sunflower-like symmetrical fashion commenced to move in a clockwise direction (images III−VI). The circular motion began at ca. −1.2 V (the threshold potential), followed by a transient jumping of the pink $BTD^{\bullet-}$ species from the vicinity of the mercury sphere to the bulk solution (such jumping of the pink $BTD^{\bullet-}$ species can be seen around the HSMPE in the images IV and V as indicated by arrows, where a dense curvature of the pink $BTD^{\bullet-}$ could be observed), i.e., the circular motion is triggered by a threshold potential. In image V, which was captured at the time of 0.2 s after the jumping of the $BTD^{\bullet-}$ species, a peculiar clockwise circular motion of the pink $BTD^{\bullet-}$ species centering the HSMPE sphere (this motion can be compared with the expression of a moving fan) can be seen. In this case, the circular motion was accompanied with CVACO (the CV data is not shown). Finally, the color of the $BTD^{\bullet-}$ species is completely diminished, and the obtained image of the HSMPE is essentially similar to image I.

As is seen above, the circular motion occurs during the reoxidation of $BTD^{\bullet-}$ to BTD (anodic process), but its origin is not clear yet. In addition, the similar circular motion in the opposite direction ought to be expected during the cyclic voltammetric reduction of BTD to pink $BTD^{\bullet-}$ (cathodic process). Here, we extensively carried out the visualization experiments with the HSMPE at some restricted conditions, for example, changing the position of the reference electrode with respect to the position of the electric contact of the mercury pool and measuring the videos with the HSMPE that was prepared by filling partially the cavity of the Teflon base with liquid mercury. During the anodic process at the HSMPE, the circular motion of pink $BTD^{\bullet-}$ was found to take place in the anticlockwise direction when the position of the reference electrode was fixed around the electric contact of the mercury pool. On the other hand, the clockwise circular motion of the pink $BTD^{\bullet-}$ was retained when the reference electrode was placed far away from the electric contact (actually, in cases of the above-mentioned video measurements at the HMDE and HSMPE, the position of the reference electrode was far away from the so-called electric contact). At the intermediate positions of the reference electrode, the directions of the motion of the pink $BTD^{\bullet-}$ were random. It has been known that the potential on the mercury electrode is not homogeneously distributed over the whole surface and the potential on a portion of the mercury electrode depends on the position of the reference electrode with respect to position of the electric contact of the mercury pool.[15,26,29] Thus, the asymmetry in the potential distribution on the mercury electrode seems to direct the circular motion of the pink $BTD^{\bullet-}$ (discussed later). By fixing the position of the reference electrode far away from the electric contact of the partially filled HSMPE, interestingly, the expected anticlockwise circular motion was observed during the reduction of BTD to pink $BTD^{\bullet-}$ (cathodic process), whereas this motion switched to the clockwise one when the potential of the CV measurement was switched for the reoxidation of pink $BTD^{\bullet-}$ to BTD (anodic process) (video B). We could successfully visualize the expected anticlockwise circular motion during the reduction of colorless BTD to pink $BTD^{\bullet-}$ by setting up the experimental condition that the initially formed pink $BTD^{\bullet-}$ did not get out from the cavity of the partially filled HSMPE before ending the potential scan for the cathodic process. In addition, the mercury pool of the partially filled HSMPE was observed to come out and go into the cavity during the reduction and oxidation processes, respectively, suggesting the existence of the expansion and shrinking phenomena of the mercury pool during the redox process as mentioned above.

Similar eccentric phenomena with the HMDE could be also seen by using other electrochromic reactions, for example, 9,10-diphenylanthracene (DPA), azobenzene, and tris(2,2′-bipyridine) ruthenium(II) dichloride, or in other solvents such as *N*,*N*-dimethylformamide (DMF). In addition, the upward and downward streaming and the circular motion during the redox reaction of the $BTD/BTD^{\bullet-}$ couple at the HMDE/DMSO solution interface could be observed by the eyes through a magnifying glass. On the contrary, the video obtained at the spherical Pt electrode showed that the electrogenerated pink $BTD^{\bullet-}$ homogeneously diffused and paled in the electrode vicinity during the reduction and oxidation processes, respectively (the data is not shown here), but the above-mentioned eccentric phenomena did not occur. Moreover, a homogeneous distribution and decay of the color formed during the $BTD/BTD^{\bullet-}$ redox reaction was found at the Pt disk electrode arranged at an angle of ca. 110° to the CCD−camera probe in the solution containing moving dust particles. Therefore, the observed circular motion of the pink $BTD^{\bullet-}$ at the HMDE originates neither from the gravitational field and the thermal convection (that may arise from the light irradiation during the measurement of video) nor the specific properties of the solvent and redox couple (e.g., adsorption), that is, the circular motion is a self-insisting phenomenon in nature. In this connection, it can be understood that the negatively charged species ($BTD^{\bullet-}$) discharges (oxidizes) at the moving (i.e., downwardly streamed) and charged liquid HMDE surface, resulting in the instability at the interface and the oscillation on the anodic peak (Figure 1). Thus, the origin of CVACO is not simple. However, this observation could be a model for the other systems in which the instabilities result from the movement of a charged species (particle) over a charged liquid surface in motion, for example, electroosmotic flow in a biochannel.[1−3]

The formal potential of the $BTD/BTD^{\bullet-}$ redox couple (−1.32 V) is more negative than the PZC of the HMDE in a DMSO solution containing 0.1 M TEAP [−0.27 V vs Ag/AgCl/NaCl (saturated)].[26] According to the classical concept of the polarographic maxima of the first kind,[15,26−29] the upward and downward streaming phenomena of the HMDE occur during the reduction and oxidation processes, respectively, at potentials more negative than the PZC (the detail is given in the Supporting Information). In Figure 4 are schematically shown the electrocapillary curve, reduction, and oxidation processes at potentials negative to the PZC (a), a cross section of an HMDE (b), upward (c) and downward (d) streaming phenomena, circular motion (e), and the sectional views of the HSMPE (f) and the partially filled HSMPE (g and h) with the direction of the circular motion. Santhanam and Bard[15] have first explained CVACO observed for the redox reaction of DPA in DMF solution based on the concept that CVACO occurs due to the downward streaming of the HMDE and its adjoining solution. Later, the similar explanation has been also proposed by Ginzburg et al.[20,21] for the inverted peaks and current oscillations in cyclic voltammetry,

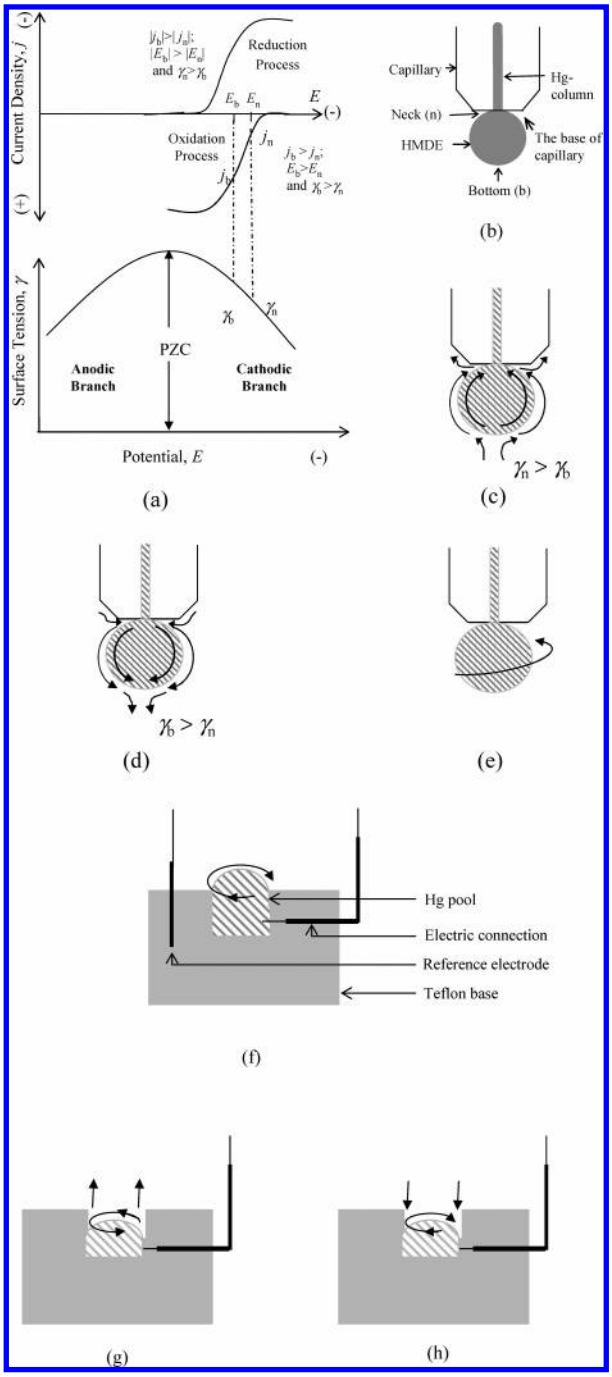

Figure 4. Schematic representations of (a) an electrocapillary curve (ECC) and electrochemical processes (i.e., reduction and oxidation), (b) a cross section of HMDE, (c) upward and (d) downward streaming of the HMDE surface and its adjoining solution, (e) a circular motion in the solution adjoining to the HMDE surface, (f) a sectional view of a hemispherical mercury pool electrode (HSMPE), and (g and h) a sectional view of the partially filled HSMPE. The potential of zero charge (PZC) and the potentials negative and positive than the PZC on the ECC are indicated. The relationships among current density (j), potential (E), and surface tension (γ) with respect to the electrochemical processes at potentials negative than the PZC are also shown. The arrows shown by the curvatures in the panels (e−h) indicate the direction of the circular motion, and upward and downward arrows shown in the panels (g) and (h) represent the directions of the expansion and shrinking of the mercury pool during the reduction and reoxidation processes, respectively.

that is, the uneven polarization of the HMDE and the specific adsorption of the reactant and/or the electrogenerated product induce tangential movements of the HMDE surface and its adjoining solution and ultimately cause CVACO.[20] However, these cannot satisfactorily explain the CVACO, which is "a bundle of current spikes" (Figure 1), because the streaming phenomena generally cause smooth maxima on the rising part of the limiting current region at a dropping mercury electrode.[29] Therefore, in the case of CV obtained at the HMDE, the streaming maximum is expected to merge with the peak current. In fact, the smooth cathodic and current-oscillating anodic peaks were observed, respectively (Figure 1), when the upward (Figure 4c) and downward streaming (Figure 4d) can be expected. In this circumstance, some previously reported phenomena that are characteristic of the mercury electrodes, but may not be clearly understood by the classical concept of the maxima of the first kind, can be noted: the pulsation called "beating mercury heart"[30] and the distortion of the shape of mercury electrodes,[28,31] and cellular convections at a mercury pool electrode/aqueous solution.[34,35]

In 1978, the theories of the polarographic streaming maxima of the first kind given by Frumkin and Levich,[37,38] Stackelberge,[39] and Bauer[40] have been developed critically by Aogaki et al.[41,42] They have analyzed the maximum current of the first kind in terms of the momentum equations for the liquid metal and liquid electrolyte, diffusion equation for active ionic species, and some electrochemical conditions. They have proposed that the maximum current is a manifestation of different electrochemical and hydrodynamical instabilities originating from incessant, small, and random disturbance (perturbation) about the surface of the mercury electrode. Such small perturbations are endlessly amplified to macroscopic instabilities by their coupling in a cyclic chain: surface tension → surface motion → bulk motion → diffusional mass transport → surface electrochemical potential → surface tension.[41] Moreover, this theory can also explain the other features observed at the mercury electrodes that can be explained by the classical theory, for example, the streaming effects on the current−potential curve lessen as the potential of an electrochemical process approaches the PZC (i.e., the so-called surface tension difference approaches zero),[26,29] and they increase as the concentrations of redox species and electrolyte increase and decrease, respectively.[42] Furthermore, this theory has been claimed to be a well-fitted one with the characteristics of the experimental polarographic maxima in aqueous solutions and molten salt systems.[41,42]

Although the origin of the circular motion observed during CVACO cannot be explained by the classical theory, it can be satisfactorily understood by considering the factors governing the maxima of the first kind presented by the modern theory.[41,42] According to the classical mechanics of the motion, only a unique force (e.g., in this case, downward streaming) cannot cause a circular motion because the circular motion has two components named centrifugal and centripetal forces. Therefore, the result of the above-mentioned infinitesimal perturbations presented in the theory given by Aogaki et al. possibly creates the observed circular motion of the pink $BTD^{\bullet -}$.

In summary, the cyclic coupling of various infinitesimally small instabilities resulting from the downward streaming (mechanical), inhomogeneous distributions of potentials and reoxidizable species through the neck to the bottom of the HMDE (electrochemical), and the tangential transport of the species located in the vicinity of the neck to the bottom (hydrodynamical) may cause the observed circular motion. Thus, the observation of this circular motion verifies the modern concept for the polarographic maxima of the first kind[41,42] and may open a new route to study the vortex (i.e., instability) in a liquid electrode/liquid electrolyte interface. On the other hand, a series of the upward, downward, and circular motions can be

repeatedly created simply by cycling the electrode potential to switch on the redox reaction. Thus, this system could be regarded as a microtransducer for a mechanical amplification system triggered by an electrochemical redox reaction.

Acknowledgment. The present work was financially supported by grant-in-aids for scientific research on priority areas (no. 417), scientific research (no. 12875164), and scientific research (A) (no. 10305064) to T. Ohsaka, from the Ministry of Education, Culture, Sports, Science, and Technology of the Japanese Government (Monbu-Kagakusho), and Venture Business Laboratory Program at TIT. The authors thank Professor R. Aogaki at Polytechnic University, Japan for his helpful discussion about the experimental results based on the modern theory proposed by him for the polarographic streaming maxima. M.M.I. gratefully acknowledges the Government of Japan for a Monbu-Kagakusho Scholarship and appreciates the financial support of the KATOH Science Foundation, Japan.

Supporting Information Available: Videos obtained at the HMDE and HSMPE (AVI), classical theory of polarographic streaming maxima of the first kind, and references. This material is available free of charge via the Internet at http://pubs.acs.org.

References and Notes

(1) Herrada, M. A.; Barrero, A. *Phys. Rev. E* **2002**, *66*, 03631-1.
(2) Thamida, S. K.; Chang, H.-C. *Phys. Fluids* **2002**, *14*, 4315.
(3) Stroock, A. D.; Weck, M.; Chiu, D. T.; Huck, W. T. S.; Kenis, P. J. A.; Ismagilov, R. F.; Whitesides, G. M. *Phys. Rev. Lett.* **2000**, *84*, 3314.
(4) Morrow, F. J. *J. Chem. Educ.* **1971**, *48*, 368.
(5) Fahidy, T. Z.; Gu, Z. H. In *Modern Aspects of Electrochemistry*; White, R. E., Bockris, J. O'M., Conway, B. E., Eds.; Plenum Press: Now York, 1995; Vol. 27.
(6) Wojtowitcz, J. In *Modern Aspects of Electrochemistry*, Bockris, J. O'M., Conway, B. E., Eds.; Plenum Press: New York, 1973; Vol. 8.
(7) Pagitsas, M.; Sazou, D. *J. Electroanal. Chem.* **1999**, *471*, 132.
(8) Strasser, P.; Eiswirth, M.; Koper, M. T. M. *J. Electroanal. Chem.* **1999**, *478*, 50.
(9) Pimienta, V.; Etchenique, R.; Buhse, T. *J. Phys. Chem. A* **2001**, *105*, 10037.
(10) Franck, F. U. *Angew. Chemie* **1978**, *17*, 1.
(11) Gao, J.; Ren, J.; Yang, W.; Liu, X.; Yang, H.; Li, Q.; Deng, H. *J. Electroanal. Chem.* **2002**, *520*, 157.
(12) Kakiuchi, T.; Chiba, M.; Sezaki, N.; Nakagawa, M. *Electrochem. Commun.* **2002**, *4*, 701.
(13) Islam, M. M.; Saha, M. S.; Okajima, T.; Ohsaka, T. *J. Electroanal. Chem.* **2005**, *577*, 145.
(14) Philp, R. H., Jr.; Layloff, T.; Adams, R. N. *J. Electrochem. Soc.* **1964**, *111*, 1189.
(15) Santhanam, K. S. V.; Bard, A. J. *J. Am. Chem. Soc.* **1966**, *88*, 2669.
(16) Guyon, A. L.; Klein, L. J.; Goken, D. M.; Peters, D. G. *J. Electroanal. Chem.* **2002**, *526*, 134.
(17) Chen, T.-Y. R.; Anderson, M. R.; Peters, D. G. *J. Electroanal. Chem.* **1987**, *222*, 257.
(18) Aravamuthan, S.; Kalidas, C.; Venkatachalam, C. S. *J. Electroanal. Chem.* **1984**, *171*, 293.
(19) Ortiz, M. E.; Nunez-Vergara, L. J.; Squella, J. A. *J. Electroanal. Chem.* **2002**, *519*, 46.
(20) Ginzburg, G.; Becker, J. Y.; Lederman, E. *Electrochim. Acta* **1981**, *26*, 851.
(21) Becker, J. Y.; Ginzburg, G.; Willner, I. *J. Electroanal. Chem.* **1980**, *108*, 355.
(22) Che, Y.; Okajima, T.; Nakamura, Y.; Tokuda, K.; Ohsaka, T. *Chem. Lett.* **1998**, 97.
(23) Wu, J. F.; Okajima, T.; Tokuda, K.; Ohsaka, T. *Electrochemistry* **2000**, *68*, 277.
(24) Saha, M. S.; Ohsaka, T. *Jpn. J. Deuterium Sci.* **2000**, *9*, 35.
(25) Saha, M. S.; Che, Y.; Okajima, T.; Kiguchi, T.; Nakamura, Y.; Tokuda, K.; Ohsaka, T. *J. Electroanal. Chem.* **2001**, *496*, 61.
(26) Islam, M. M.; Okajima, T.; Ohsaka, T. *J. Phys. Chem. B* **2004**, *108*, 19425.
(27) Saha, M. S.; Okajima, T.; Ohsaka, T. *J. Phys. Chem. B* **2002**, *106*, 4457.
(28) Islam, M. M.; Okajima, T.; Ohsaka, T. *Electrochem. Commun.* **2004**, *6*, 556.
(29) Bauer, H. H. In *Electroanalytical Chemistry*, Bard, A. J., Ed.; Marcel Dekker Inc.: New York, 1975; Vol. 8, p 169.
(30) Keizer, J.; Rock, P. A.; Lin, S.-W. *J. Am. Chem. Soc.* **1979**, *101*, 5637.
(31) Smolin, S.; Imbihl, R. *J. Phys. Chem.* **1996**, *100*, 19055.
(32) O'Brien, R. N.; Dieken, F. P. *Can. J. Chem.* **1976**, *54*, 403.
(33) Leja, J.; O'Brien, R. N. *Nature* **1966**, *210*, 1217.
(34) Sato, M.; Aogaki, R. *Electrochim. Acta* **1995**, *40*, 2921.
(35) Makino, T.; Morioka, K.; Aogaki, R. *J. Electroanal. Chem.* **1985**, *190*, 261.
(36) The time marked by 00:00:00:00 on the video data means the onset of the potential scan, and for example, the time 00:00:13:00 indicates the elapse of time (i.e., 13 s) for the cathodic potential scan.
(37) Levie, R. D. *J. Electroanal. Chem.* **1965**, *9*, 311.
(38) Levich, V. G. *Physicochemical Hydrodynamics*; Prentice Hall: New York, 1962.
(39) Stackelberg, M. V.; Doppelfeld, R. *Adv. Polym.* **1960**, *1*, 68.
(40) Bauer, H. H. *Electrochim. Acta* **1973**, *18*, 427.
(41) Aogaki, R.; Kitazawa, K.; Fueki, K.; Mukaibo T. *Electrochim. Acta* **1978**, *23*, 867.
(42) Aogaki, R.; Kitazawa, K.; Fueki, K.; Mukaibo, T. *Electrochim. Acta* **1978**, *23*, 875.